THE JOURNAL OF BIOLOGICAL CHEMISTRY VOL. 284, NO. 39, pp. 26749–26757, September 25, 2009

Isoform Specificity of the Na/K-ATPase Association and Regulation by Phospholemman*

Received for publication, July 21, 2009 Published, JBC Papers in Press, July 28, 2009, DOI 10.1074/jbc.M109.047357

Julie Bossuyt[‡1], **Sanda Despa**[‡1], **Fei Han**[§], **Zhanjia Hou**[¶], **Seth L. Robia**[¶], **Jerry B. Lingrel**[‖], **and Donald M. Bers**[‡2]

From the [‡]*Department of Pharmacology, University of California, Davis, California 95616, the* [§]*Department of Pathology, Feinberg School of Medicine, Northwestern University, Chicago, Illinois 60611, the* [¶]*Department of Physiology, Loyola University Chicago, Maywood, Illinois 60153, and the* [‖]*Department of Molecular Genetics, Biochemistry, and Microbiology, University of Cincinnati, Cincinnati, Ohio 45267*

Phospholemman (PLM) phosphorylation mediates enhanced Na/K-ATPase (NKA) function during adrenergic stimulation of the heart. Multiple NKA isoforms exist, and their function/regulation may differ. We combined fluorescence resonance energy transfer (FRET) and functional measurements to investigate isoform specificity of the NKA-PLM interaction. FRET was measured as the increase in the donor fluorescence (CFP-NKA-α1 or CFP-NKA-α2) during progressive acceptor (PLM-YFP) photobleach in HEK-293 cells. Both pairs exhibited robust FRET (maximum of 23.6 ± 3.4% for NKA-α1 and 27.5 ± 2.5% for NKA-α2). Donor fluorescence depended linearly on acceptor fluorescence, indicating a 1:1 PLM:NKA stoichiometry for both isoforms. PLM phosphorylation induced by cAMP-dependent protein kinase and protein kinase C activation drastically reduced the FRET with both NKA isoforms. However, submaximal cAMP-dependent protein kinase activation had less effect on PLM-NKA-α2 *versus* PLM-NKA-α1. Surprisingly, ouabain virtually abolished NKA-PLM FRET but only partially reduced co-immunoprecipitation. PLM-CFP also showed FRET to PLM-YFP, but the relationship during progressive photobleach was highly nonlinear, indicating oligomers involving ≥3 monomers. Using cardiac myocytes from wild-type mice and mice where NKA-α1 is ouabain-sensitive and NKA-α2 is ouabain-resistant, we assessed the effects of PLM phosphorylation on NKA-α1 and NKA-α2 function. Isoproterenol enhanced internal Na^+ affinity of both isoforms ($K_{½}$ decreased from 18.1 ± 2.0 to 11.5 ± 1.9 mM for NKA-α1 and from 16.4 ± 2.5 to 10.4 ± 1.5 mM for NKA-α2) without altering maximum transport rate (V_{max}). Protein kinase C activation also decreased $K_{½}$ for both NKA-α1 and NKA-α2 (to 9.4 ± 1.0 and 9.1 ± 1.1 mM, respectively) but increased V_{max} only for NKA-α2 (1.9 ± 0.4 *versus* 1.2 ± 0.5 mM/min). In conclusion, PLM associates with and modulates both NKA-α1 and NKA-α2 in a comparable but not identical manner.

Cardiac Na/K-ATPase (NKA)[3] regulates intracellular Na^+, which in turn affects intracellular Ca^{2+} and contractility via Na^+/Ca^{2+} exchange. Members of the F*X*YD family of small, single membrane-spanning proteins, including phospholemman (PLM) and the NKA γ-subunit (1), have emerged recently as tissue-specific regulators of NKA. PLM is the only F*X*YD protein known to be highly expressed in cardiac myocytes and is also unique within the family in that it is phosphorylated at two or more sites by cAMP-dependent protein kinase (PKA) and protein kinase C (PKC) (2, 3). In the heart, PLM is a major phosphorylation target for both PKA and PKC.

Co-immunoprecipitation experiments have demonstrated that PLM is physically associated with NKA (4–8), and this is not affected by PLM phosphorylation (6, 7). We have shown recently (9) that PLM and NKA are in very close proximity, such that fluorescence resonance energy transfer (FRET) occurs. PLM phosphorylation by either PKA or PKC reduces the FRET significantly, suggesting that although PLM and NKA are not physically dissociated upon phosphorylation, their interaction is altered. PLM inhibits NKA (4, 8, 10, 11), mostly by reducing the affinity of the pump for internal Na^+. PLM phosphorylation relieves this inhibition and thus mediates the enhancement of NKA function by α- and β-adrenergic stimulation in mouse ventricular myocytes (10, 11).

There are multiple NKA isoforms in cardiac myocytes. NKA-α1 is the dominant, ubiquitous isoform, whereas NKA-α2 and NKA-α3 are present in relatively small amounts and in a species-dependent manner (12). For instance, the adult rodent heart expresses NKA-α1 and NKA-α2, although dogs and monkeys do not have the NKA-α2 subunit (13). In humans all three NKA-α isoforms can be detected (14). It has been suggested that NKA-α2 and NKA-α3 are located mainly in the T-tubules, at the junctions with the sarcoplasmic reticulum, where they could regulate local Na^+/Ca^{2+} exchange and thus cardiac myocyte Ca^{2+}. There is rather convincing evidence supporting such a model in the smooth muscle (15). However, things are less clear in the heart. The functional density of NKA-α2 is significantly higher in the T-tubules (*versus* external sarcolemma) in cardiac myocytes from both rats (16, 17) and mice (18), but their precise localization with respect to the junctions with the sarcoplasmic reticulum is not known. Based on Ca^{2+} transients from heterozygous NKA-$\alpha1^{+/-}$ and NKA-$\alpha2^{+/-}$ mice, James *et al.* (19) concluded that NKA-α2 is

* This work was supported, in whole or in part, by National Institutes of Health Grants HL-30077 and HL-81526 (to D. M. B.). This work was also supported by American Heart Association Grant 0735084N (to S. D.).

[1] Both authors contributed equally to this work.

[2] To whom correspondence should be addressed: Dept. of Pharmacology, University of California, Genome Bldg. 3511, Davis, CA 95616-8636. Tel.: 530-752-6517; Fax: 530-752-7710; E-mail: dmbers@ucdavis.edu.

[3] The abbreviations used are: NKA, Na/K-ATPase; PLM, phospholemman; PLB, phospholamban; FRET, fluorescence resonance energy transfer; SR, sarcoplasmic reticulum; ISO, isoproterenol; CFP, cyan fluorescent protein; YFP, yellow fluorescent protein; PDBu, phorbol 12,13-dibutyrate; SERCA, sarco(endo)plasmic/reticulum Ca-ATPase; SBFI, sodium benzofuran isophthalate; SBFI-AM, SBFI-acetoxymethyl ester.

involved in cardiac myocyte Ca^{2+} regulation, whereas NKA-α1 is not. Further support for this idea came from the observation that replacing mouse NKA-α2 with a low affinity mutant leads to a loss of glycoside inotropy (20), and increased expression of NKA-α2 decreased the Na^+/Ca^{2+} exchange current and Ca^{2+} transients (21). However, other findings challenge the preferential role of NKA-α2 in regulating intracellular Ca^{2+} and contractility. Moseley *et al.* (22) showed that NKA-$\alpha1^{+/-}$ mice were severely compromised, and Dostanic *et al.* (23) showed that NKA-α1 is also physically and functionally associated with the Na^+/Ca^{2+} exchanger.

In this context, it is important to determine whether NKA-α1 and NKA-α2 interact differently with PLM. The data available so far on this are contradictory. We have found (7) that NKA-α1, NKA-α2, and NKA-α3 isoforms co-immunoprecipitate PLM, both unphosphorylated and phosphorylated, in rabbit heart. In contrast, Silverman *et al.* (8) reported that NKA-α1 but not NKA-α2 co-immunoprecipitate with PLM in ventricular myocytes from guinea pig. The functional data are also contradictory. PLM was found to reduce the affinity for Na^+ of both NKA-α1 and NKA-α2 isoforms in a heterologous expression system (4), whereas Silverman *et al.* (8) reported that forskolin-induced PLM phosphorylation results in a higher NKA-α1-mediated current and no change in the current generated by NKA-α2.

Here we used two methods to investigate whether the interaction and functional effects of PLM on NKA are NKA-α isoform-specific. First, we used FRET to assess the interaction between PLM-YFP and CFP-NKA-α1/CFP-NKA-α2 transfected in HEK-293 cells and how PLM phosphorylation by PKA and PKC affects this interaction. Second, we measured NKA function in myocytes isolated from wild-type (WT) mice and mice where NKA isoforms have swapped ouabain affinities (SWAP; NKA-α1 is ouabain-sensitive, whereas NKA-α2 is ouabain-resistant) (23). In this way we could test the effect of β-adrenergic stimulation separately on NKA-α1 and NKA-α2 isoforms in the native myocyte environment, as an indicator of the functional interaction with PLM. Our results indicate that NKA-α1 and NKA-α2 interact similarly with PLM, and this interaction is equally affected by PLM phosphorylation.

EXPERIMENTAL PROCEDURES

Constructs—The PLM-CFP and PLM-YFP constructs (with CFP or YFP attached to the intracellular C terminus) were generated as described previously (9). Rat CFP-NKA-α1 and CFP-NKA-α2 fusion proteins (where CFP is attached at the intracellular N terminus) were generated by subcloning the NKA isoform sequence into the pECFP C1 vector (with the A206K monomerization mutation; Clontech) using the HindIII and XbaI sites. The fusion proteins were confirmed by sequencing and Western blot analysis.

Culture and Transfection of HEK-293 Cells—HEK-293 cells (American Type Culture Collection, Manassas, VA) were cultured in Dulbecco's modified Eagle's medium with 5% fetal bovine serum and penicillin/streptomycin on laminin-coated coverslips. After 24 h, cells (~60% confluency) were co-transfected with plasmids encoding CFP/YFP fusion construct cDNAs of PLM, rat NKA-α1, and rat NKA-α2 using the mammalian transfection kit (Stratagene); 10 μg of DNA (3:1 ratio) was used for NKA:PLM experiments and 3 μg of DNA (1:1 ratio) for PLM:PLM experiments, which yielded ~60 and ~40% transfection efficiencies for PLM and NKA, respectively (with >80% co-expression). Cells were then cultured for another 24 h prior to experiments.

Generation of SWAP Mice and Cardiac Myocyte Isolation—Mice expressing ouabain-sensitive NKA-α1 and ouabain-resistant NKA-α2 (SWAP) were developed by mating mice with ouabain-sensitive NKA-α1 isoform ($\alpha1^{SS}\alpha2^{SS}$) (23) with mice having an ouabain-resistant NKA-α2 isoform ($\alpha1^{RR}\alpha2^{RR}$) (20), as described previously (23). The ouabain-sensitive mouse NKA-α1 isoform was obtained by introducing the R111Q and D122N amino acid substitutions into the first extracellular domain of this isoform. The Gln-111 and Asn-122 residues are naturally present in the high affinity human and sheep NKA-α1 isoforms and were shown to confer sensitivity to cardiac glycosides (24, 25). The ouabain-resistant mouse NKA-α2 isoform was obtained by introducing the L111R and N122D amino acid substitutions. The Arg-111 and Asp-122 residues are naturally present in the low affinity rodent NKA-α1 isoforms. The L111R and N122D amino acid substitutions reduced by 1000-fold the ouabain affinity of the sheep NKA-α1 isoform without altering its enzymatic activity (24, 25). The expression and tissue distribution of NKA-α1 and NKA-α2 isoforms are normal in the SWAP animals, and the mutations did not alter the enzymatic activity of the two isoforms (23). All animal protocols were approved by the animal welfare committees at the University of Cincinnati or University of California, Davis.

Isolation of mouse ventricular myocytes was as described previously (26). Briefly, SWAP mice and age-matched WT littermates (3–4 months age) were anesthetized in a gas chamber with 3–5% isoflurane (100% O_2). Hearts were excised quickly, mounted on a gravity-driven Langendorff perfusion apparatus, and perfused with minimum essential medium (Sigma) supplemented with insulin and pyruvic acid. After 2–3 min of perfusion in nominally Ca^{2+}-free minimum essential medium, hearts were digested by perfusion with 0.8 mg/ml collagenase (type B; Roche Applied Science) in the presence of 20 μM Ca^{2+} and 1 mg/ml taurine. When the heart became flaccid (7–12 min), ventricular tissue was removed, dispersed, and filtered, and myocyte suspensions were rinsed several times. Until use, myocytes were kept at room temperature in minimum essential medium containing 100 μM Ca^{2+} and 1.3 mg/ml taurine. Myocytes were used for experiments within 6 h after isolation.

Immunoprecipitation—NKA-α subunits and PLM were immunoprecipitated as described previously (4, 7), using the PLM-C2 antibody. Cardiac myocytes were treated with 10 mM ouabain or vehicle for 10 min prior to lysing in solubilization buffer (±10 mM ouabain) containing 6 mg/ml *n*-dodecyl octaethylene glycol monoether detergent ($C_{12}E_8$; Calbiochem) and (in mmol/liter) 140 NaCl, 25 imidazole, and 1 EDTA (pH 7.3). The extract from this solubilization step (30 min at 4 °C) was diluted 1:1 with detergent-free buffer to 1 mg/ml cardiac protein and centrifuged for 30 min at 20,000 × *g* at 4 °C to remove debris (pellet Na/K-ATPase was very low). Cell lysates were incubated with the primary antibody overnight at 4 °C with end-over-end rotation. Immune complexes were collected after

2 h of incubation with 40 μl of secondary goat anti-rabbit IgG antibody covalently bound to agarose beads (Sigma). Immunoprecipitates were collected by centrifugation at 10,000 × *g* for 10 min at 4 °C and washed five times with solubilization buffer containing 0.05% $C_{12}E_8$. After the final wash, the pellet was resuspended in sample buffer. Samples were centrifuged at 10,000 × *g* for 10 min, and supernatants were saved to load on the gel. Samples were then size-fractionated on 10% SDS-PAGE. Proteins were transferred to a 0.20-μm nitrocellulose membrane (NaF and $NaVO_3$ were added to transfer buffer). Immunoblots were blocked with 5% milk in Tris-buffered saline/Tween and then incubated overnight at 4 °C with primary antibody as follows: NKA-α1 (1:1000 dilution, clone C464.6 from Upstate); NKA-α2 (1:1000 dilution; Chemicon), and custom PLM-C2 (1:1000 dilution) (7, 9). After incubation with the horseradish peroxidase-labeled secondary antibody, blots were developed using enhanced chemiluminescence (Pierce Supersignal). All signals were recorded using a UVP EpichemII darkroom imaging system for quantification and captured on film for representation. All experiments were performed in duplicate.

Fluorescence Resonance Energy Transfer (FRET) Measurements—FRET was measured using the acceptor photobleaching method. When FRET is present, the photobleaching of the acceptor (YFP) prevents FRET with a consequent increase in the direct emission from the donor (CFP). Here YFP was progressively photobleached using the following protocol: 100-ms acquisition of CFP image, 40-ms acquisition of YFP image, followed by repeated 10-s exposure to YFP-selective photobleaching (504/12 nm excitation). Fluorescence imaging was performed with an inverted microscope equipped with a 1.49 NA objective and a back-thinned CCD camera (iXon 887, Andor Technology, Belfast, Northern Ireland). Image acquisition and acceptor photobleaching were automated with custom software macros in MetaMorph (Molecular Devices Corp., Downingtown, PA) that controlled motorized excitation/emission filter wheels (Sutter Instrument Co., Novato, CA) with filters for CFP (excitation 427/10 nm, emission 472/30 nm) and YFP (excitation 504/12 nm, emission 542/27) (Semrock, Rochester, NY).

For these experiments, we used cells where the base-line YFP/CFP ratio was high, in the range where differences in this ratio did not alter the measured FRET. This ensures that the maximum FRET values obtained here were the maximum obtainable for the CFP/YFP pair. FRET efficiency was calculated from the fluorescence intensity of the CFP donor before ($F_{\mathrm{Prebleach}}$) and after ($F_{\mathrm{Postbleach}}$) acceptor-selective photobleaching, according to the following relationship: $E = 1 - (F_{\mathrm{Prebleach}}/F_{\mathrm{Postbleach}})$. The distance between the CFP-YFP pair was calculated from the FRET efficiency using the Förster equation; $R = R_0 \cdot ((1 - E)/E)^{1/6}$, where R_0 is the Förster distance (5.3 nm for the CFP-YFP pair (27)).

$[Na]_i$ Measurements—Isolated myocytes were plated on laminin-coated coverslips and loaded with SBFI-AM (10 μmol/liter, for 90–120 min; Invitrogen) as described previously (10). SBFI was allowed to de-esterify for 20 min in normal Tyrode's solution containing the following (in mmol/liter): 140 NaCl, 4 KCl, 1 $MgCl_2$, 10 glucose, 5 HEPES, and 1 $CaCl_2$ (pH 7.4). SBFI was alternately excited at 340 and 380 nm (F_{340} and F_{380}) using an Optoscan monochromator (Cairn Research, Faversham, UK), and fluorescence was collected at 535 ± 20 nm. F_{340}/F_{380} was calculated after background subtraction and converted to $[Na^+]_i$ by calibration at the end of each experiment in the presence of 10 μmol/liter gramicidin and 100 μmol/liter strophanthidin.

NKA Isoform-mediated Na^+ Efflux—The Na^+ flux through NKA-α1 and NKA-α2 was determined as the rate of $[Na^+]_i$ decline that was mediated by the ouabain-insensitive NKA isoform in WT and SWAP mice, respectively. Myocytes were Na^+-loaded by inhibiting NKA in a K^+-free solution containing (mmol/liter) the following: 145 NaCl, 2 EGTA, 10 HEPES, and 10 glucose (pH 7.4) (28). $[Na^+]_i$ decline was measured upon pump reactivation in a solution containing (mmol/liter) the following: 140 triethanolamine-Cl, 4 KCl, 1 $MgCl_2$, 2 EGTA, 10 HEPES, and 10 glucose (pH 7.4). The ouabain-sensitive NKA isoform was completely blocked with 20 μM ouabain present throughout the experiment. Because cell volume does not change with this protocol (28), $[Na^+]_i$ decline reflects Na^+ efflux. The rate of $[Na^+]_i$ decline ($-d[Na^+]_i/dt$) was plotted *versus* $[Na^+]_i$ and fitted with $-d[Na^+]_i/dt = V_{\max}/(1 + (K_{0.5}/[Na]_i)^{n\mathrm{Hill}})$, where $V_{\max}$ is the maximum Na^+ extrusion rate of the respective NKA isoform; $K_{½}$ is the $[Na^+]_i$ for the half-maximal activation of the pump, and n_{Hill} is the Hill coefficient.

Statistical Analysis—Data are expressed as means ± S.E. Statistical discriminations were performed with Student's *t* test (paired when appropriate) with $p < 0.05$ considered significant.

RESULTS

Interaction between PLM-YFP and CFP-NKA-α1/CFP-NKA-α2 as Revealed by FRET—We have shown previously (9) that there is robust FRET between canine NKA-α1, tagged with CFP, and PLM-YFP transfected into HEK-293 cells. Here we used rat CFP-NKA-α1 and CFP-NKA-α2 to assess the interaction with PLM-YFP (canine). The PLM sequences in dog and rat are highly homologous (70%), especially in the cytosolic domain (more than 80% homology) (29). All constructs were targeted to the plasma membrane in HEK-293 cells, whether expressed independently or together (data not shown) as we previously showed in confocal images for PLM-YFP and CFP-NKA-α1 (9). Note that the images in Fig. 1*A* are nonconfocal, for the progressive gradual photobleach experiments. We measured FRET as an increase in the fluorescence of the donor (CFP-NKA-α1/CFP-NKA-α2) upon photobleaching the acceptor (PLM-YFP). PLM-YFP was progressively photobleached, and every 10 s we acquired a CFP and a YFP image (Fig. 1). The progressive photobleaching resulted in an exponential decline of YFP emission and a concomitant increase in the fluorescence of CFP attached to both NKA-α1 and NKA-α2 (Fig. 1). The donor fluorescence intensity increased to a similar maximum of 123.6 ± 3.4 and 127.5 ± 2.5% for NKA-α1 and NKA-α2, indicating FRET efficiencies of 0.19 and 0.21, respectively. Based on these values, we estimated the intermolecular CFP-YFP distance as 6.8 nm for the PLM-NKA-α1 pair and 6.6 nm for the PLM-NKA-α2 pair. Thus, PLM is equally close to and could interact with both NKA-α1 and NKA-α2 in the plasma membrane.

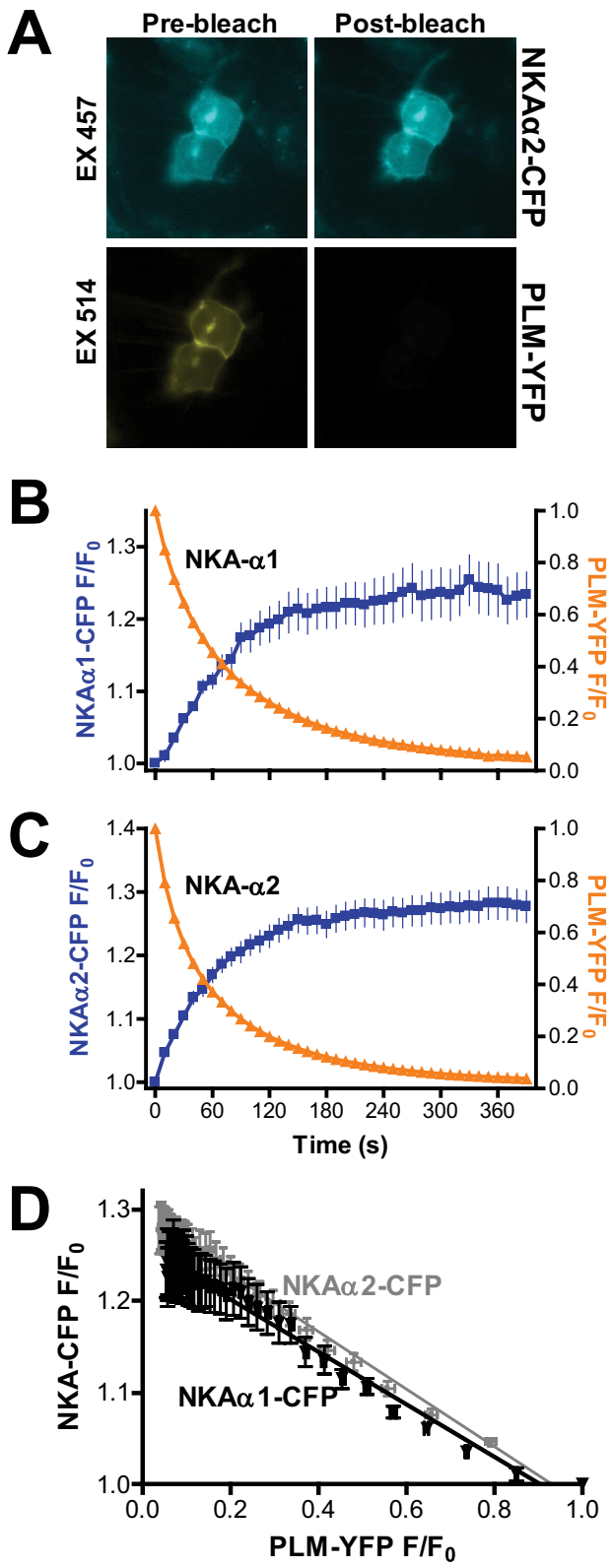

FIGURE 1. **FRET between CFP-NKA-α1/CFP-NKA-α2 and PLM-YFP transfected in HEK-293 cells detected with a progressive acceptor photobleaching protocol.** *A,* CFP-NKA-α2 and PLM-YFP epifluorescence images before starting the photobleaching (*Pre-bleach*) and at 400 s during photobleaching (*Post-bleach*). The intensity of YFP emission decreases exponentially, whereas the CFP fluorescence increases with the photobleaching of YFP, indicating the existence of FRET. *B* and *C,* mean data for the CFP- NKA and PLM-YFP fluorescence during the progressive acceptor photobleaching protocol for cells transfected with PLM and CFP-NKA-α1 (*B,* 24 cells) or CFP-NKA-α2 (*C,* 40 cells). *D,* change in the donor (PLM-YFP) *versus* acceptor (CFP-NKA) fluorescence during the progressive acceptor photobleach. The relationship is linear for both NKA-α1 and NKA-α2.

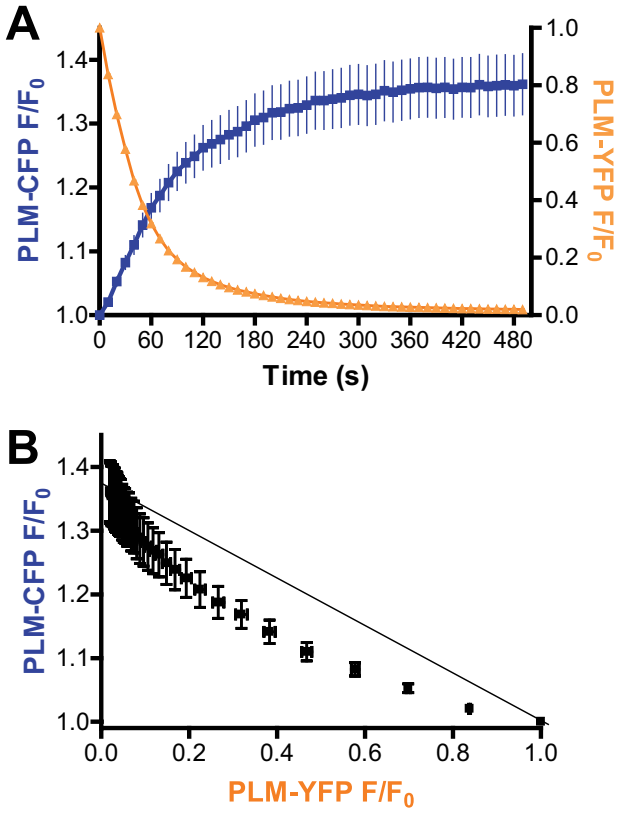

FIGURE 2. **Detection of FRET between PLM-CFP and PLM-YFP.** *A,* relative change in the PLM-CFP and PLM-YFP fluorescence during the progressive acceptor photobleaching protocol. *B,* relative change in the donor (PLM-YFP) *versus* acceptor (PLM-CFP) fluorescence during the progressive acceptor photobleach.

In an oligomeric complex, the energy transfer efficiency is sensitive to the number of molecules within the oligomer, such that the stoichiometry of the complex can be derived from the curvature of the donor *versus* acceptor fluorescence relationship (30). Thus, we replotted (Fig. 1*D*) the data in Fig. 1, *B* and *C,* as the change in the fluorescence of the donor (NKA-CFP) *versus* that of the acceptor (PLM-YFP) during the progressive photobleaching of PLM-YFP (and thus reduction in the availability of the acceptor). Note that PLM availability is not limiting in these experiments because we focused on cells with a high base-line YFP/CFP ratio (so that differences in the ratio did not alter the measured FRET, in other words we obtained maximal FRET values). For both NKA isoforms the relationship was linear, indicating a 1:1 stoichiometry of the PLM-NKA interaction (30, 31).

Acceptor photobleaching revealed that there is also robust FRET between PLM-CFP and PLM-YFP (Fig. 2*A*, cells expressing only endogenous NKA). We have shown previously that unlabeled PLM could largely prevent the increase in PLM-CFP signal upon PLM-YFP photobleaching, and thus the FRET between PLM-CFP and PLM-YFP is not because of the nonspecific CFP-YFP interaction. The donor fluorescence increased to a maximum of 136 ± 5%. In contrast to NKA-CFP/PLM-YFP,

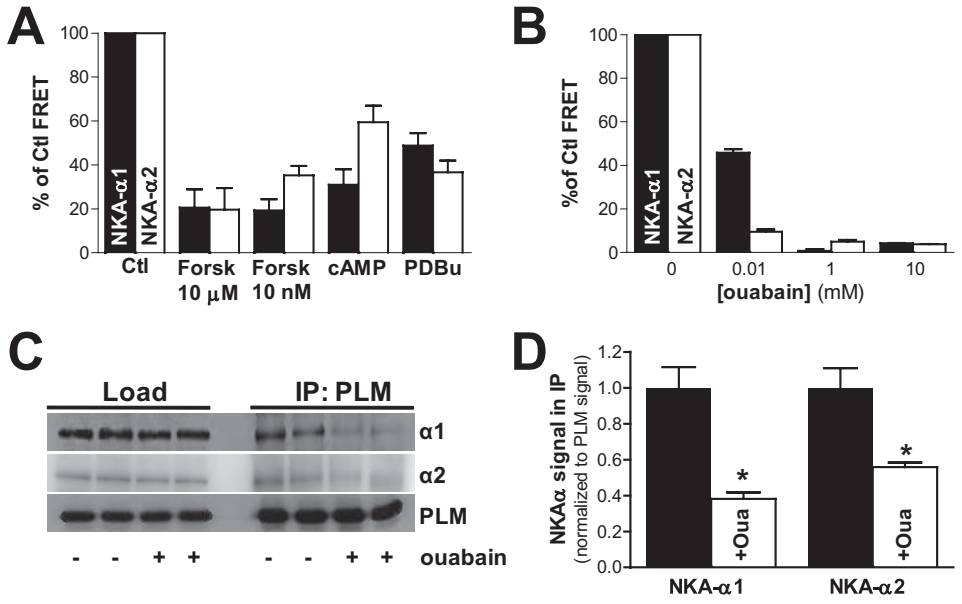

FIGURE 3. **Effect of PLM phosphorylation and NKA inhibition on the FRET between CFP-NKA-α1/CFP-NKA-α2 and PLM-YFP.** *A,* effect of high (*Forsk*, 10 μM; mean of 47 and 20 cells for NKA-α1 and NKA-α2, respectively) and low concentrations (10 nM, mean of 37 and 47 cells for NKA-α1 and NKA-α2, respectively) of forskolin, 8-bromo-cAMP (10 μM, mean of 35 and 49 cells for NKA-α1 and NKA-α2, respectively), and 100 nM PDBu ($n = 52$ and 58 for NKA-α1 and NKA-α2, respectively); *Ctl,* control. *B,* effect of various concentrations of ouabain on the FRET between PLM-NKA-α1 and PLM-NKA-α2. More than 14 cells were used for each experimental condition. *C* and *D,* effect of ouabain treatment (10 mM for 10 min) on PLM co-immunoprecipitation with NKA-α1 and NKA-α2. The NKA isoform signal (at 110 kDa) was quantified in the immunoprecipitate (*IP:PLM column*) and normalized to the corresponding PLM signal (at 10 kDa). Ouabain (*Oua*) did not affect the total NKA-α1 and NKA-α2 amount (*Load column*).

the relationship between the fluorescence of the donor and the acceptor is nonlinear (Fig. 2*B*). The observed deviation from linearity supports the model that PLM can form homo-oligomers of at least three molecules (32).

Effect of PLM Phosphorylation and Ouabain on FRET with NKA-α1/NKA-α2—We have shown previously that PLM phosphorylation by PKA and PKC enhances the NKA activity (10, 11) and drastically reduces the FRET between canine NKA-α1 and PLM (9). Here we used the progressive acceptor (PLM-YFP) photobleaching method described above to investigate the effect of PLM phosphorylation on the interaction with rat NKA-α1 and NKA-α2. PLM phosphorylation upon PKA activation with 10 μM forskolin considerably reduced the FRET with both NKA isoforms. With forskolin, the maximum increase in donor fluorescence was only 21 ± 8% (for NKA-α1) and 20 ± 10% (for NKA-α2) of the increase observed under control conditions (Fig. 3*A*). However, submaximal PKA activation with a lower concentration of forskolin (10 nM) or 10 μM 8-bromo-cAMP had a smaller effect on the FRET between PLM and NKA-α2 as compared with the PLM-NKA-α1 pair (Fig. 3*A*). This suggests that the local signaling complexes may be different for the two NKA isoforms. Activation of PKC (by 100 nM PDBu) also significantly reduced the FRET to 49 ± 6% of the maximum under control conditions for NKA-α1 and to 37 ± 5% of the control for NKA-α2 (Fig. 3*A*).

Interestingly, application of 1–10 mM ouabain completely prevented the increase in the CFP fluorescence upon photobleaching of PLM-YFP for both NKA isoforms (Fig. 3*B*). A lower ouabain concentration (10 μM, expected to mainly affect the ouabain-sensitive NKA-α2) almost abolished FRET between PLM and NKA-α2, with less effect on NKA-α1 (Fig. 3*B*). This effect was phosphorylation-independent, as pretreatment with staurosporine (10 μM) did not significantly affect the FRET (data not shown). Interestingly, ouabain also considerably reduced the amounts of NKA-α1 and NKA-α2 that co-immunoprecipitate with PLM in adult rat cardiac myocytes (Fig. 3, *C* and *D*).

Effect of ISO and PDBu on NKA-α1 and NKA-α2-mediated Na^+ Efflux in Mouse Ventricular Myocytes—In the mouse, NKA-α1 and NKA-α2 can be separated based on their different ouabain affinities. The dominant NKA-α1 isoform is ouabain-resistant, whereas NKA-α2 is ouabain-sensitive. Based on prior work (18), ouabain concentrations around 10 μM should completely block NKA-α2 while leaving the NKA-α1 activity at 92% of the maximum. Thus, one can measure directly the transport properties of NKA-α1 when NKA-α2 is blocked. The Na^+ transport characteristics of NKA-α2 can then be determined by subtracting the contribution of NKA-α1 from the total pump-mediated transport. With this approach, the contribution of the small NKA-α2 component is derived by subtracting two large numbers, which makes such a measurement prone to large errors (18). To circumvent this problem, we used transgenic mice where NKA isoforms have swapped ouabain affinities (NKA-α1 is ouabain-sensitive, and NKA-α2 is ouabain-resistant; SWAP mice) (23). The ouabain-sensitive component (NKA-α2 in WT mice and NKA-α1 in SWAP mice) was completely blocked with 20 μM ouabain, and we measured the Na^+ dependence of the rate of Na^+ extrusion mediated by the ouabain-insensitive NKA isoform (NKA-α1 in WT and NKA-α2 in SWAP mice).

Myocytes were Na^+-loaded by incubation in K^+-free solution, containing 20 μM ouabain, to block NKA (Fig. 4). Then the ouabain-resistant NKA isoform was reactivated by re-admission of 4 mmol/liter $[K^+]_o$ (and removal of extracellular Na^+), and the time course of $[Na^+]_i$ decline was measured. The protocol was repeated in the presence of 1 μmol/liter ISO (Fig. 4). When two consecutive control runs are done, the resulting Na^+ efflux is highly reproducible (10). $[Na^+]_i$ decline in each case was numerically differentiated, and $-d[Na^+]_i/dt$ was plotted as a function of $[Na^+]_i$. Na^+ efflux through the ouabain-resistant NKA isoform (NKA-α1 in WT and NKA-α2 in SWAP mice) was calculated as the difference between the Na^+ efflux measured in the presence of 20 μM ouabain (*i.e.* when the ouabain-sensitive NKA isoforms are blocked) and that in the presence of 10 mM ouabain (when all NKA isoforms are blocked; leaving only outward Na^+ leak). The outward Na^+ leak represented

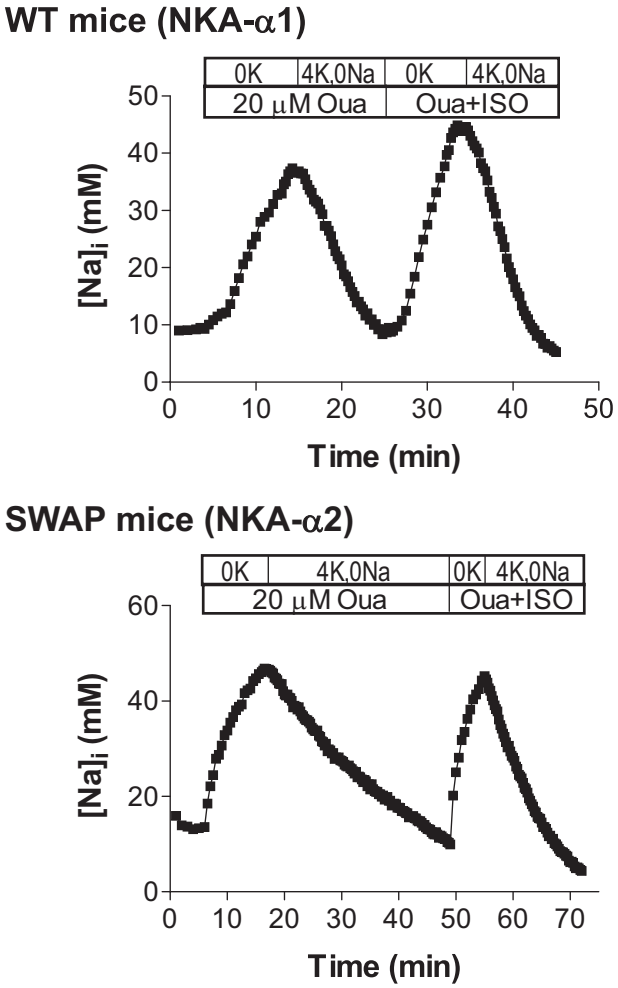

FIGURE 4. **Measurement of NKA-α1- and NKA-α2-mediated Na^+ efflux in intact mouse myocytes.** The ouabain-sensitive component (*top*, NKA-α2 in WT mice; *bottom*, NKA-α1 in SWAP mice) was completely blocked with 20 μM ouabain (*Oua*), present throughout the experiment, and we measured the Na^+ dependence of the rate of Na^+ extrusion mediated by the ouabain-insensitive NKA isoform. The ouabain-insensitive NKA was first blocked (*0K*, 145 Na^+ external solution) causing $[Na^+]_i$ loading, then reactivated in *4K,0Na* solution. The protocol was repeated with 1 μM ISO present. ISO was applied 10 min before activating the pump and then throughout measuring the NKA function.

about 20% of the Na^+ efflux measured in the presence of 20 μM ouabain for myocytes from SWAP mice and about 5% for the WT mice (data not shown).

Fig. 5 shows average data for the effect of ISO on the $[Na^+]_i$ dependence of NKA-α1 and NKA-α2. Data were fit with a Hill expression to derive the V_{max}, K_m, and n_H values (Fig. 5*A*). There was no significant difference in the apparent K_m value for Na^+ between NKA-α1 and NKA-α2 (18.1 $\pm$ 2.0 mM *versus* 16.4 $\pm$ 2.5 mM; Fig. 5*C*). The maximum Na^+ extrusion rate (V_{max}) was 5.9 $\pm$ 0.6 mM/min for NKA-α1 and 1.7 $\pm$ 0.7 mM/min for NKA-α2 (Fig. 5*B*). Assuming that 20 μM ouabain completely blocks the high affinity component and has little effect on the low affinity NKA isoform, this indicates that NKA-α2 contribution to Na^+ efflux under maximal conditions represents 22 $\pm$ 12% from the total NKA-mediated Na^+ efflux. This is within the range previously reported in rodent hearts (16–18, 33). Isoproterenol (1 μM) significantly increased the affinity for internal Na^+ of both NKA-α1 (K_m decreased to 11.5 $\pm$ 1.9 mM) and NKA-α2 (K_m decreased to 10.4 $\pm$ 1.5 mM) with no significant effect on V_{max}. Thus, β-adrenergic stimulation enhances the activity of both NKA-α1 and NKA-α2 isoforms to a similar extent. Because this effect is mediated by PLM phosphorylation (10), it suggests that NKA-α1 and NKA-α2 interact similarly with PLM, and PLM phosphorylation can similarly regulate NKA activity.

We have performed parallel experiments to investigate the effect of PLM phosphorylation by PKC, activated by PDBu (300 nM), and measuring the $[Na^+]_i$ dependence of NKA-α1 and NKA-α2 (Fig. 6). PDBu decreased the K_m value for internal Na^+ of both NKA-α1 (from 16.6 $\pm$ 1.0 to 9.4 $\pm$ 1.0 mM) and NKA-α2 (from 15.3 $\pm$ 3.1 to 9.1 $\pm$ 1.1 mM). However, PDBu significantly increased the V_{max} value for the NKA-α2 (from 1.2 $\pm$ 0.5 to 1.9 $\pm$ 0.4 mM/min, $n = 6$, $p = 0.038$, paired t test) but had no effect on the NKA-α1 V_{max}. Thus, there are some differences in the way PLM phosphorylation by PKC affects NKA-α1 and NKA-α2 in mouse ventricular myocytes.

DISCUSSION

NKA Isoform Specificity of the NKA-PLM Interaction—There are multiple NKA isoforms in cardiac myocytes, and they may play different functional roles based on their specific localization and/or modulation. There is controversy regarding the isoform specificity of NKA regulation by PLM, a member of the FXYD family of tissue-specific NKA modulators that is highly expressed in the heart. Here we combined FRET and functional measurements to show that PLM interacts with and modulates both NKA-α1 and NKA-α2 isoforms to a similar extent.

We found robust FRET between PLM-YFP and both CFP-NKA-α1 and CFP-NKA-α2, indicating that PLM is in the close proximity (<9 nm) of both NKA isoforms. Moreover, the maximum amount of FRET, and thus the estimated PLM-NKA intermolecular distance, was similar for the two isoforms. PLM has multiple phosphorylation sites at its cytosolic C terminus. PKA phosphorylates PLM at Ser-68, and PKC phosphorylates the Ser-68 and Ser-63 sites. PLM phosphorylation by PKA (forskolin and 8-bromo-cAMP) or PKC (PDBu) drastically reduced the FRET with both NKA isoforms. At saturating concentrations (10 μM), forskolin nearly abolished the FRET for both NKA-α1 and NKA-α2 (about 80% FRET reduction). However, PLM and NKA remain associated upon PLM phosphorylation by PKA, as revealed by co-immunoprecipitation (7, 34), and this might explain the residual FRET observed in the presence of forskolin.

Submaximal concentrations of forskolin (10 nM) and 8-bromo-cAMP had a smaller effect on the FRET between PLM-NKA-α2 than on PLM-NKA-α1. This suggests that there might be some subtle differences in the way PLM phosphorylation at Ser-68 affects the interaction with the two NKA isoforms. Alternatively, the PKA or the phosphatase activity near NKA-α2 may be different from that in the vicinity of NKA-α1, resulting in a lower phosphorylation level of PLM associated with NKA-α2 *versus* that of PLM associated with NKA-α1. This is plausible as NKA-α1 and NKA-α2 have different membrane localizations, with NKA-α2 concentrated in the T-tubules and NKA-α1 uniformly distributed between T-tubules and external sarcolemma (16–18).

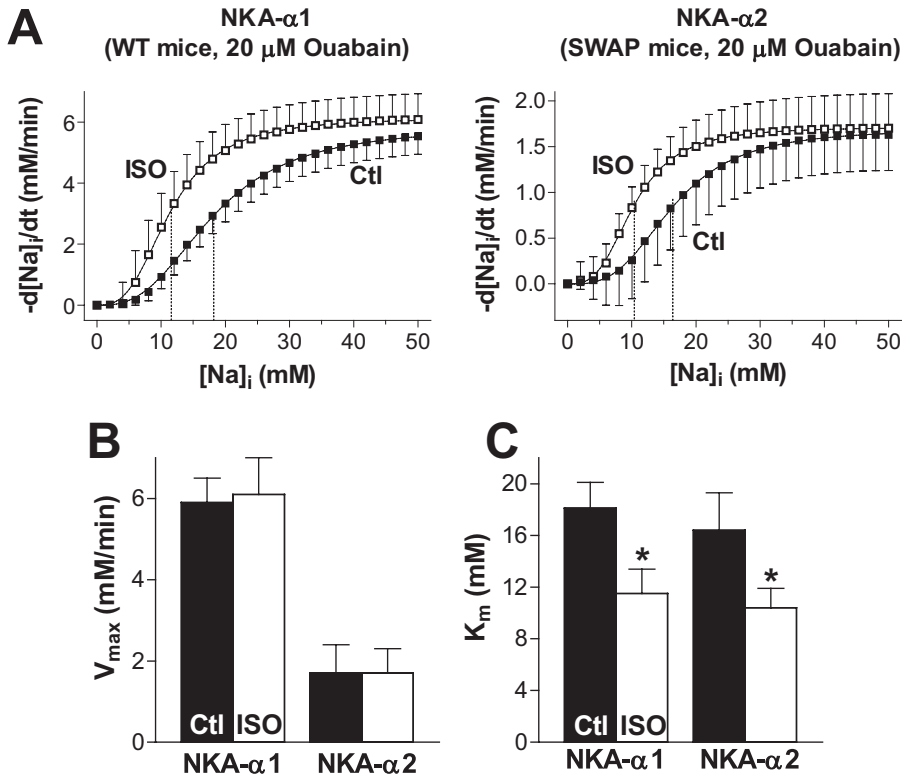

FIGURE 5. **Effect of ISO (1 μM) on Na^+ efflux through NKA-α1 and NKA-α2.** *A,* $[Na^+]_i$ dependence of Na^+ extrusion by NKA-α1 (the ouabain-sensitive Na^+/K^+ pump in WT mice, $n = 9$ cells, 6 hearts) and NKA-α2 (in SWAP mice, $n = 8$ cells, 6 hearts) with and without 1 μM ISO. *B,* maximum Na^+ extrusion rate, V_{max}, of NKA-α1 and NKA-α2, with and without ISO. *C,* $[Na^+]_i$ for the half-maximal activation of the pump, $K_{1/2}$, of NKA-α1 and NKA-α2, with and without ISO.

We and others (4, 8, 10, 11, 35) have previously shown that PLM inhibits NKA, and PLM phosphorylation relieves this inhibition. This is similar to the way PLB affects the sarco-(endo)plasmic/reticulum Ca-ATPase (SERCA), a close structural relative of NKA. Thus, PLM phosphorylation mediates the enhancement of NKA function by α- and β-adrenergic stimulation in cardiac myocytes. Here we found that PLM phosphorylation by PKA upon activation of β-adrenergic receptors with saturating concentrations of ISO (1 μM) increases the pump affinity for internal Na^+ for both NKA-α1 and NKA-α2 isoforms to a similar extent and has no effect on the maximum transport rate in mouse ventricular myocytes. These data compare very well to recent results obtained in a heterologous expression system (34). Our data are different from previous reports in guinea pig myocytes (8, 36), where β-adrenergic stimulation increased the maximum pump current generated by the NKA-α1 isoform and had no effect on the NKA-α2 (the affinity for internal Na^+ was not determined in these studies). This might indicate species-dependent differences in the way PLM phosphorylation at Ser-68 affects NKA function.

PKC activation by PDBu and subsequent PLM phosphorylation at Ser-63 and Ser-68 increased the affinity for internal Na^+ of both NKA-α1 and NKA-α2 isoforms. In a previous study (11) we found that PLM phosphorylation by PKC increased V_{max}, without significant change in Na^+ affinity. It is not clear why no $K_{1/2}$ effect was seen in that study, but we have detected $K_{1/2}$ effects of PKC activation on NKA activity in rabbit ventricular myocytes and also with heterologous NKA and PLM expression in HeLa cells (37, 38). PDBu also significantly increased the maximum transport rate for the NKA-α2 with no effect on NKA-α1, in agreement with previous data in guinea pig myocytes (36) and heterologous expression systems (34). Although PDBu seemed to reduce more the mean FRET between PLM and NKA-α2 than for PLM-NKA-α1, the difference was not statistically significant.

Ouabain Abolishes NKA-PLM FRET—Interestingly, NKA blockade with ouabain practically abolished the FRET between PLM and either NKA-α1 and NKA-α2 and resulted in partial dissociation of the PLM·NKA complex as assessed by co-immunoprecipitation. This is a remarkable and novel result. The partial decrease (~50%) in co-immunoprecipitation suggests that ouabain decreases the affinity of PLM for NKA. The observation that FRET is virtually abolished by ouabain, with evidence of retained PLM-NKA interaction, implies that there is some profound modification in NKA structure in a way that the fluorophores are much further apart (or strictly re-oriented). More study will be required to provide further structural interpretation.

Stoichiometry of NKA·PLM and PLM·PLM Complexes—FRET (this study and Ref. 9) and co-immunoprecipitation experiments (4–8, 34) have indicated that PLM forms a complex with NKA but also forms homo-oligomers in the plasma membrane. The progressive acceptor photobleaching experiments done here allowed us to derive the stoichiometry of the NKA·PLM and PLM·PLM complexes. The fluorescence of the donor increased linearly as a function of the decreasing acceptor fluorescence for both NKA-α1·PLM and NKA-α2·PLM, indicating a 1:1 stoichiometry of these complexes (30, 31). This is in agreement with co-immunoprecipitation data for the NKA·PLM complex (4, 7) as well as for the complex formed by NKA with other F*X*YD proteins (39).

For the PLM·PLM complex, the relationship between the fluorescence of the donor and that of the acceptor was nonlinear. This suggests that PLM may exist in the membrane as a homo-oligomer with three or more molecules. This is in agreement with structural data indicating that PLM may exist in the membrane as a tetramer (32). It is thus possible that PLM forms channels, as originally proposed by Moorman *et al.* (40), although the physiological significance of such channels is unclear. An alternative explanation is that multiple pools of PLM exist in the membrane. As a monomer, PLM can associate with and modulate NKA (both NKA-α1 and NKA-α2) and maybe also the Na^+/Ca^{2+} exchanger (41). The homo-oli-

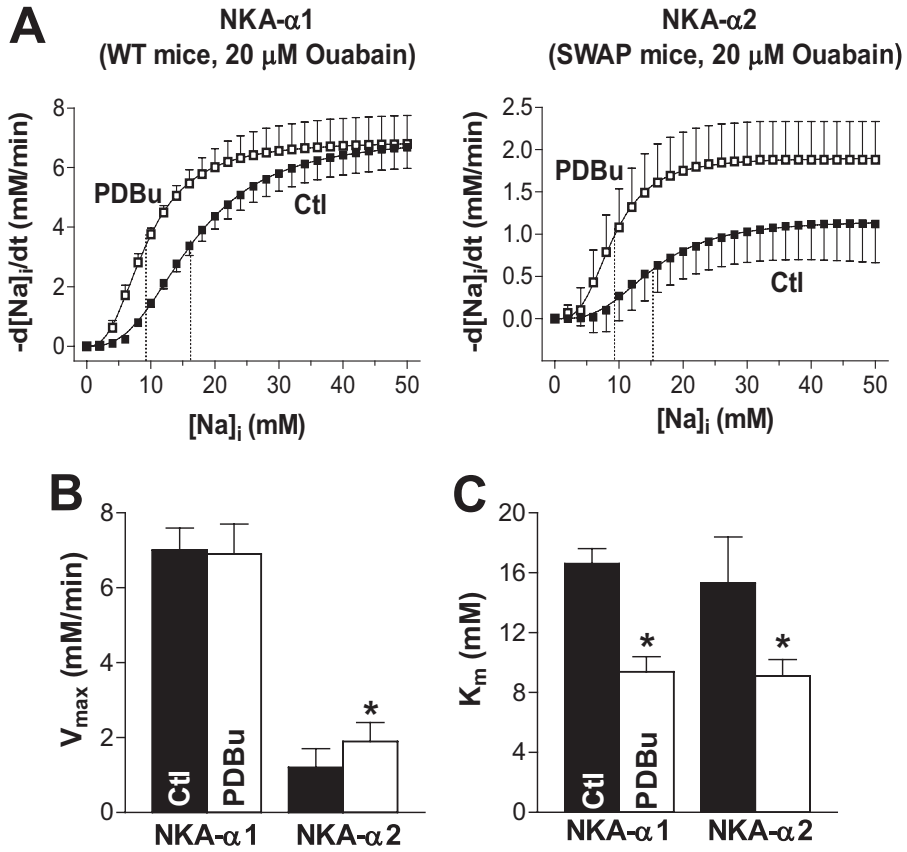

FIGURE 6. **Effect of PDBu (300 nM) on Na^+ efflux through NKA-α1 and NKA-α2.** *A*, $[Na^+]_i$ dependence of Na^+ extrusion by NKA-α1 ($n = 5$ cells, 3 hearts) and NKA-α2 ($n = 6$ cells, 3 hearts) with and without 300 nM PDBu. *B*, maximum Na^+ extrusion rate, V_{max} of NKA-α1 and NKA-α2, with and without PDBu. *C*, $[Na^+]_i$ for the half-maximal activation of the pump, $K_{1/2}$, of NKA-α1 and NKA-α2, with and without PDBu.

gomers may serve as a storage pool for PLM (in equilibrium with monomers). However, it is not known whether a significant fraction of endogenous PLM exists as homo-oligomers in cardiac myocytes. Thus, PLM oligomerization may also be simply a result of overexpression. Nevertheless, these results further emphasize the similarity between NKA -PLM and SERCA-PLB interactions, as phospholamban also exists both as monomers, which associate with SERCA (42, 43), and as inactive pentamers (44).

Analogies to SERCA and Phospholamban Complexes—PLB forms very stable homo-pentamers, even in SDS-PAGE. PLM also multimerizes (≥3; Fig. 2) and structural evidence suggests tetramers (32), but our results cannot distinguish between trimer and pentamer. Unlike PLB pentamers, PLM oligomers are not stable in detergent and not readily apparent in SDS-PAGE. The maximal PLM-PLM FRET here (26%) is rather modest for a complex with multiple FRET acceptors, consistent with widely separated cytoplasmic domains. The PLM oligomer quaternary conformation may be analogous to the "pinwheel" structure of the PLB pentamer (45, 46), in which cytoplasmic domains closely associate with the membrane surface (47) and point away from the center of the complex. A similar model for PLM would also be consistent with the high resolution structure of the PLM monomer, which revealed an L-shaped architecture (48). The maximal PLM-PLM FRET here (26%) is less than that recently reported for PLB-PLB using the same strategy (45%; see Ref. 31); this may reflect the greater length of the cytoplasmic domain of PLM compared with PLB (35 and 29 amino acids, respectively). Additional FRET studies can be envisioned that would directly test the conformation and affinity of the PLM oligomer, as was previously done for PLB (31, 49).

The maximal extent of FRET between CFP-SERCA and YFP-PLB was reported to be 30%, using experiments highly parallel to those of this study. Assuming a significant portion of the NKA is bound to PLM, the observed maximal NKA-PLM FRET efficiency (~20%) reflects a distance of >60 Å. Such a long transfer distance is compatible with the CFP fused to the N terminus of NKA and the YFP fused to PLM being on opposite sides of the regulatory complex, in agreement with recent structural data for renal NKA and γ-subunit (FXYD2) (50). This is consistent with substantial structural parallelism between the PLM·NKA and PLB·SERCA complexes.

In summary, we have combined FRET and functional measurements to show that PLM associates with and modulates both NKA-α1 and NKA-α2 isoforms to a similar extent. PLM phosphorylation by PKA and PKC affects the interaction with NKA-α1 and NKA-α2 in a comparable but not identical manner, suggesting that there might be some subtle differences in the way PLM associates with and regulates the two NKA isoforms.

Acknowledgments—We thank Dr. Jody Martin and Karl Hench for help with the construct generation and Dr. Jaime DeSantiago and Junaid Ahsan for myocyte preparation.

REFERENCES

1. Sweadner, K. J., and Rael, E. (2000) *Genomics* **68,** 41–56
2. Presti, C. F., Jones, L. R., and Lindemann, J. P. (1985) *J. Biol. Chem.* **260,** 3860–3867
3. Palmer, C. J., Scott, B. T., and Jones L. R. (1991) *J. Biol. Chem.* **266,** 11126–11130
4. Crambert, G., Fuzesi, M., Garty, H., Karlish, S., and Geering, K. (2002) *Proc. Natl. Acad. Sci. U.S.A.* **99,** 11476–11481
5. Feschenko, M. S., Donnet, C., Wetzel, R. K., Asinovski, N. K., Jones, L. R., and Sweadner, K. J. (2003) *J. Neurosci.* **23,** 2161–2169
6. Fuller, W., Eaton, P., Bell, J. R., and Shattock, M. J. (2004) *FASEB J.* **18,** 197–199
7. Bossuyt, J., Ai, X., Moorman, J. R., Pogwizd, S. M., and Bers, D. M. (2005) *Circ. Res.* **97,** 558–565
8. Silverman, B. Z., Fuller, W., Eaton, P., Deng, J., Moorman, J. R., Cheung, J. Y., James, A. F., and Shattock, M. J. (2005) *Cardiovasc. Res.* **65,** 93–103
9. Bossuyt, J., Despa, S., Martin, J. L., and Bers, D. M. (2006) *J. Biol. Chem.*

281, 32765–32773
10. Despa, S., Bossuyt, J., Han, F., Ginsburg, K. S., Jia, L. G., Kutchai, H., Tucker, A. L., and Bers, D. M. (2005) *Circ. Res.* **97,** 252–259
11. Han, F., Bossuyt, J., Despa, S., Tucker, A. L., and Bers, D. M. (2006) *Circ. Res.* **99,** 1376–1383
12. McDonough, A. A., Zhang, Y., Shin, V., and Frank, J. S. (1996) *Am. J. Physiol.* **270,** C1221–C1227
13. Hensley, C. B., Azuma, K. K., Tang, M. J., and McDonough, A. A. (1992) *Am. J. Physiol.* **262,** C484–C492
14. Sweadner, K. J., Herrera, V. L., Amato, S., Moellmann, A., Gibbons, D. K., and Repke, K. R. (1994) *Circ. Res.* **74,** 669–678
15. Juhaszova, M., and Blaustein, M. P. (1997) *Proc. Natl. Acad. Sci. U.S.A.* **94,** 1800–1805
16. Despa, S., and Bers, D. M. (2007) *Am. J. Physiol. Cell Physiol.* **293,** C321–CC327
17. Swift, F., Tovsrud, N., Enger, U. H., Sjaastad, I., and Sejersted, O. M. (2007) *Cardiovasc. Res.* **75,** 109–117
18. Berry, R. G., Despa, S., Fuller, W., Bers, D. M., and Shattock, M. J. (2007) *Cardiovasc. Res.* **73,** 92–100
19. James, P. F., Grupp, I. L., Grupp, G., Woo, A. L., Askew, G. R., Croyle, M. L., Walsh, R. A., and Lingrel, J. B. (1999) *Mol. Cell* **3,** 555–563
20. Dostanic, I., Lorenz, J. N., Schultz, Jel, J., Grupp, I. L., Neumann, J. C., Wani, M. A., and Lingrel, J. B. (2003) *J. Biol. Chem.* **278,** 53026–53034
21. Yamamoto, T., Su, Z., Moseley, A. E., Kadono, T., Zhang, J., Cougnon, M., Li, F., Lingrel, J. B., and Barry, W. H. (2005) *J. Mol. Cell. Cardiol.* **39,** 113–120
22. Moseley, A. E., Huddleson, J. P., Bohanan, C. S., James, P. F., Lorenz, J. N., Aronow, B. J., and Lingrel, J. B. (2005) *Cell. Physiol. Biochem.* **15,** 145–158
23. Dostanic, I., Schultz, Jel, J., Lorenz, J. N., and Lingrel, J. B. (2004) *J. Biol. Chem.* **279,** 54053–54061
24. Price, E. M., and Lingrel, J. B. (1988) *Biochemistry* **27,** 8400–8408
25. Price, E. M., Rice, D. A., and Lingrel, J. B. (1990) *J. Biol. Chem.* **265,** 6638–6641
26. DeSantiago, J., Maier, L. S., and Bers, D. M. (2002) *J. Mol. Cell. Cardiol.* **34,** 975–984
27. Elangovan, M., Wallrabe, H., Chen, Y., Day, R. N., Barroso, M., and Periasamy, A. (2003) *Methods* **29,** 58–73
28. Despa, S., Islam, M. A., Weber, C. R., Pogwizd, S. M., and Bers, D. M. (2002) *Circulation* **105,** 2543–2548
29. Chen, L. S., Lo, C. F., Numann, R., and Cuddy, M. (1997) *Genomics* **41,** 435–443
30. Li, M., Reddy, L. G., Bennett, R., Silva, N. D., Jr., Jones, L. R., and Thomas, D. D. (1999) *Biophys. J.* **76,** 2587–2599
31. Kelly, E. M., Hou, Z., Bossuyt, J., Bers, D. M., and Robia, S. L. (2008) *J. Biol. Chem.* **283,** 12202–12211
32. Beevers, A. J., and Kukol, A. (2006) *Protein Sci.* **15,** 1127–1132
33. Ishizuka, N., Fielding, A. J., and Berlin, J. R. (1996) *Jpn. J. Physiol.* **46,** 215–223
34. Bibert, S., Roy, S., Schaer, D., Horisberger, J. D., and Geering, K. (2008) *J. Biol. Chem.* **283,** 476–486
35. Lifshitz, Y., Lindzen, M., Garty, H., and Karlish, S. J. (2006) *J. Biol. Chem.* **281,** 15790–15799
36. Gao, J., Wymore, R., Wymore, R. T., Wang, Y., McKinnon, D., Dixon, J. E., Mathias, R. T., Cohen, I. S., and Baldo, G. J. (1999) *J. Physiol.* **516,** 377–383
37. Han, F., Despa, S., Bossuyt, J., Gia, L., Tucker, A. L., and Bers, D. M. (2006) *Biophys. J.* **90,** 281a (Abstr. 1355)
38. Han, F., Bossuyt, J., Martin, J., and Bers, D. M. (2008) *Biophys. J.* **94,** 144a (Abstr. 658)
39. Lindzen, M., Gottschalk, K. E., Füzesi, M., Garty, H., and Karlish, S. J. (2006) *J. Biol. Chem.* **281,** 5947–5955
40. Moorman, J. R., Ackerman, S. J., Kowdley, G. C., Griffin, M. P., Mounsey, J. P., Chen, Z., Cala, S. E., O'Brian, J. J., Szabo, G., and Jones, L. R. (1995) *Nature* **377,** 737–740
41. Wang, J., Zhang, X. Q., Ahlers, B. A., Carl, L. L., Song, J., Rothblum, L. I., Stahl, R. C., Carey, D. J., and Cheung, J. Y. (2006) *J. Biol. Chem.* **281,** 32004–32014
42. Cornea, R. L., Jones, L. R., Autry, J. M., and Thomas, D. D. (1997) *Biochemistry* **36,** 2960–2967
43. Kimura, Y., Kurzydlowski, K., Tada, M., and MacLennan, D. H. (1997) *J. Biol. Chem.* **272,** 15061–15064
44. Simmerman, H. K., Collins, J. H., Theibert, J. L., Wegener, A. D., and Jones, L. R. (1986) *J. Biol. Chem.* **261,** 13333–13341
45. Robia, S. L., Flohr, N. C., and Thomas, D. D. (2005) *Biochemistry* **44,** 4302–4311
46. Traaseth, N. J., Verardi, R., Torgersen, K. D., Karim, C. B., Thomas, D. D., and Veglia, G. (2007) *Proc. Natl. Acad. Sci. U.S.A.* **104,** 14676–14681
47. Clayton, J. C., Hughes, E., and Middleton, D. A. (2005) *Biochemistry* **44,** 17016–17026
48. Teriete, P., Franzin, C. M., Choi, J., and Marassi, F. M. (2007) *Biochemistry* **46,** 6774–6783
49. Hou, Z., Kelly, E. M., and Robia, S. L. (2008) *J. Biol. Chem.* **283,** 28996–29003
50. Morth, J. P., Pedersen, B. P., Toustrup-Jensen, M. S., Sørensen, T. L., Petersen, J., Andersen, J. P., Vilsen, B., and Nissen, P. (2007) *Nature* **450,** 1043–1049